UNIVERSIDAD TÉCNICA FEDERICO SANTA MARÍA

DEPARTAMENTO DE FÍSICA

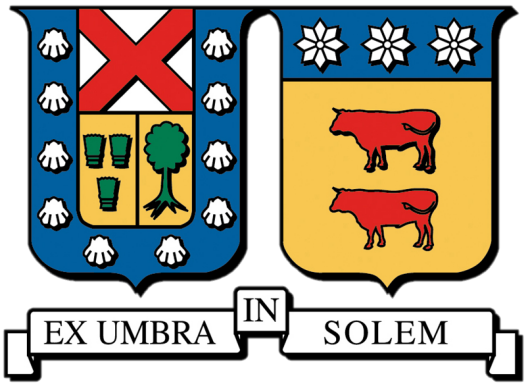

Investigating the Influence of Intracluster Filaments on Ram-Pressure Stripping in Galaxy Clusters

Javier Oñat Laurin

MEMORIA PARA OPTAR AL TÍTULO DE LA LICENCIATURA EN ASTROFÍSICA

Tutor: Yara Jaffé

August 10, 2024

Abstract

This thesis explores the potential influence of intracluster filaments on ram-pressure stripping (RPS) in galaxies, focusing on Jellyfish (JF) and Unwinding (UG) candidates identified through the citizen science project *Fishing for Jellyfish Galaxies*. We analyzed the spatial distributions of these RPS candidates relative to filaments within three galaxy clusters: A85, A1644, and Shapley. Statistical tests, including the Kolmogorov-Smirnov (K-S) and Anderson-Darling (A-D) tests, were employed to compare the distances of JF and UG candidates to the nearest filament against all other galaxies within each cluster. Our results show that, while the overall fraction of galaxies displaying RPS features is slightly higher than previously reported studies, the spatial distribution of these candidates relative to filaments does not significantly differ from the general galaxy population in the clusters examined. However, notable differences in the A1644 cluster suggest potential environmental factors affecting UG candidates differently, particularly outside of filaments. These results imply that filament proximity may not be a primary driver of RPS.

Acknowledgments

I am deeply grateful to my family for their patience and understanding, which allowed me to dedicate myself fully to this project. Your unwavering belief in my abilities kept me motivated and inspired throughout this journey.

First and foremost, I extend my sincere thanks to my advisor, Yara Jaffé, for her invaluable guidance, patience, encouragement, and insight throughout my research. Her expertise and feedback were crucial in shaping this work.

I would also like to acknowledge my colleagues and friends for their camaraderie and collaboration, particularly Constanza Céspedes and Joaquín Meza. The discussions and exchanges of ideas with you both were an enriching part of my academic journey.

Thank you all for your encouragement and support in helping me achieve this milestone.

Contents

Chapter 1

Introduction

One of the main questions in extragalactic astronomy is how galaxies form and evolve. Our current cosmological model, the Λ Cold Dark Matter (CDM) model, proposes that the large structures that first formed arose from density fluctuations in the primordial soup. These weak ripples were imposed on the otherwise uniform and rapidly expanding early Universe. As the Universe expanded and cooled, more and more cold gas began to concentrate in these density regions, which served as "seedbeds" for the formation of large-scale structures. Over 14 billion years of evolution, these ripples have been amplified to enormous proportions by gravitational forces, producing ever-growing concentrations of dark matter in which ordinary gases cool, condense and fragment to make galaxies (Springel et al. 2006). The variety of galaxies that we see today (ellipticals, irregulars and spirals) are a result of internal processes along with interactions such as mergers between ancient galaxies or with their environment. As we can appreciate the Universe grows as a hierarchical way, meaning that the massive structures accrete the lighter ones. There is vast evidence of this, and we know for fact that it did not stop growing when reached the galaxy structure instead it kept growing to form even bigger and more massive structures. These structures began to organize into a network of filaments, walls, and voids, usually called the Cosmic Web. Filaments are regions where matter is grouped, forming galaxy "highways", while voids are regions with sparse matter. At the nodes of filaments, matter is even more concentrated, giving birth to structures such as clusters and superclusters of galaxies. Walls, on the other hand, are vast, planar structures where galaxies and galaxy clusters are densely packed, creating a sort of boundary between voids. The filaments contain half of the mass in the Universe, followed by walls, voids, and clusters with 25, 15, and 10 percent, respectively. In terms of volume, the voids dominate with 78 percent of the cosmic volume, followed by walls and filaments with 18 and 6 percent (Cautun et al. 2014). Besides of these cosmic filaments we can also encounter intra-cluster filaments which are thread-like structures composed of gas and dark matter that extends between galaxies within a galaxy cluster.

There is a well known relation between the density of the environment where a galaxy resides and its morphological type (Dressler 1980). In dense environments such as galaxy clusters there is a prevalence of early-type galaxies, like ellipticals and lenticulars. These galaxies have a more spheroidal shape and little or no ongoing star formation. In contrast, in less dense environments like the field, spiral galaxies are more common. These galaxies have prominent spiral arms, a evident disk and ongoing star formation (Peng et al. 2010).

In general galaxies are structures that starts their life with a lot of gas, most of it is used as "fuel" to gave birth to new stars. These are called star forming galaxies or late-type galaxies and they are commonly bluer due to their stellar population (young stars). On the other hand, when the star formation is truncated, we named those galaxies as "quenched" or early-type galaxies and they are commonly red because they have ancient stars. This path is the most common evolution of a galaxy, from star forming to quenched. Research by (Schiminovich et al. 2010) has found that external processes or feedback mechanisms that control the gas supply are important for regulating star formation in massive galaxies.

There are several mechanisms driving galaxy evolution, which can be divided into two main groups: internal and external, as mentioned by Peng et al. 2010. Some examples of the internal mechanisms that can make a galaxy evolve are gas consumption by star formation, supernovae explosions may eject gas out of the galaxy together with stellar winds or radiation pressure, Active Galactic Nuclei (AGN) can also be causing the expelling of the gas, these are supermassive black holes at the center of the galaxies that launch powerful jets, expelling the gas of the galaxy. External mechanisms can be broadly categorized into gravitational and hydrodynamical effects, both of which can contribute to quenching a galaxy, according to (Boselli and Gavazzi 2006 ; Fossati et al. 2019). In gravitational effects we can find mergers, majors and minors, where the former occurs when two galaxies of comparable mass collide and merge, leading to significant changes in morphology, star formation rate, and the distribution of dark matter. Whereas the later involve a large galaxy merging with a much smaller one, triggering localized star formation and gradually alter the larger galaxy's structure. Tidal interactions occurs when a galaxy passes close to another galaxy or cluster causing stars and gas to be torn away from the outer regions, altering the structure and dynamics of the galaxy that is hit. When a galaxy moves through a larger one or through a dense environment can experience drag force, this process can cause the loss of momentum and eventually a merge between galaxies. Harassment also occurs in dense environments, this is defined as cumulative high-speed encounters with other galaxies provoking gravitational perturbations resulting in morphological changes and heating of the stellar and gaseous components.
Alternatively, there are also hydrodynamical interactions, as highlighted by Cortese et al. 2021, which are primarily between the gas component of different objects, whether between galaxies or within a galaxy and its surrounding medium. Gas accretion is when galaxies accrete gas from their surroundings, either from intergalactic medium (IGM) or from the circumgalactic medium (CGM), this accreted gas serve as fuel for new star formation and contribute to the growth of the galaxy. Strangulation occurs in dense environments, where galaxies can lose their ability to accrete fresh gas from their surroundings due to the hot, dense gas in a cluster or group. This generates a gravitational influence that inhibits the inflow of new gas, leading to the exhaustion of gas reserves and subsequently the cease on the star formation. Based on the research of (Vulcani et al. 2022) one of the most powerful processes influencing the gas reserves in large galaxy clusters is the removal of gas due to the pressure exerted by the intracluster medium (ICM) as galaxies move through it, this pressure imparted, is directly proportional to the local gas density of the ICM and to the square of the galaxy's velocity with respect to the ICM (Gunn and Gott 1972) and is termed ram pressure stripping (RPS). The most notable examples of this phenomenon are galaxies that display tentacles of debris with a jellyfish-like morphology, featuring extended tails of optically bright , stripped material, commonly referred to as 'jellyfish' (JF) (e.g. McPartland et al., 2016; Poggianti et al., 2016). The gas removal in cluster galaxies has been demonstrated

though observations of neutral gas (HI) in clusters galaxies (Chung et al. 2009 ; Jaffé et al. 2015). Often, there is a phase during the gas stripping where increased star formation occurs in the disk of these objects, as well as in the tails (Vulcani et al. 2022). Another phenomenon, described by Vulcani et al. 2022, involves "unwinding spiral arms" – spiral galaxies with unwound arms that exhibit a redder hue, heightened brilliance, and increased mass, indicative of intensified star formation. These galaxies might enter the cluster at an earlier stage compared to JF galaxies. Overall, RPS leads to the loss/consumption of gas from the galaxy and a subsequent decrease in overall star formation activity.

All the environmental effects mentioned can occur before galaxies enter a larger, denser environment such as a galaxy cluster. They can also take place in smaller, less dense environments like galaxy groups, indicating that the properties of galaxies observed in clusters are not solely attributed to the cluster environment but also influenced by their earlier interactions and evolution in smaller groups or subclusters (Fujita 2004). This phenomenon is referred to as preprocessing. Occurs well outside the core of rich clusters, and has been invoked to explain why the atomic gas content and the star formation activity are found suppressed at large clustercentric distances.

To understand how filaments impact the quenching of galaxies, Kotecha et al. (2022) conducted a study highlighting the importance of the intra-cluster environment and cosmic filaments in regulating star formation and galaxy evolution within clusters. Utilizing simulations, they found that deep cluster filaments delay the quenching of galaxies in hot, dense cluster environments. This delay allows cluster galaxies to continue forming stars as they move deeper into the cluster, as evidenced by an increased fraction of star-forming galaxies, a prevalence of bluer galaxies, and higher amounts of cold gas in satellites near filaments. Conversely, outside clusters, simulations show that galaxies are redder when closer to filaments. Importantly, these findings are based on simulations and have not yet been observed directly. Additionally, the cold gas fraction in these galaxies decreases as they approach filaments. This contrast highlights the role of the filaments in different environments; outside clusters filaments contributes to preprocessing whereas inside cluster filaments "shield" the galaxies from being quenched. This 'shielding' effect notably occurs close to 1 R_{200}. The analysis of this research is conducted at $z = 0$. Therefore, it does not quantify how this trend varies with cosmic time. Furthermore, it is important to remark that since this study is based on simulations, there has not been any observational study of the influence of filaments in the intra-cluster environment. Figure 1.1 from (Kotecha et al. 2022) visually represents these phenomena. The figure shows the circum-filament gas density (in green) and intra-cluster medium density (in red) with a temperature gradient indicating cooler to hotter regions. It depicts the pre-processing of galaxies in the cold gas phase at the periphery, the preservation of accretion as galaxies approach the cluster, and the quenching process inside the cluster. The figure highlights that galaxies near filaments retain more cold gas and experience reduced RPS, compared to those further from filaments, thereby illustrating the complex interactions between filaments and intra-cluster environments in galaxy evolution.

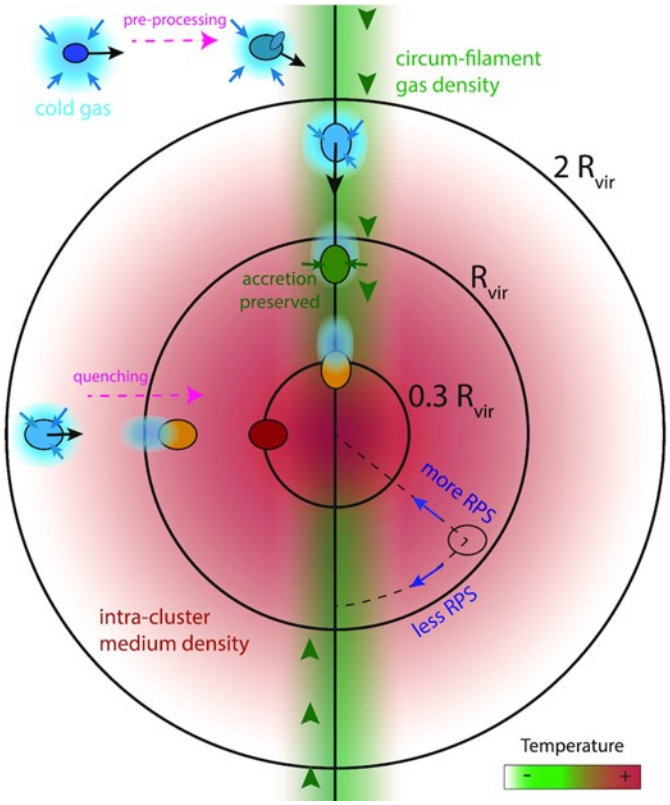

Figure 1.1: Illustration of how cosmic filaments influence galaxy evolution in clusters: Galaxies near filaments retain more cold gas and experience reduced quenching due to lower ram pressure stripping, while those further from filaments are quenched more quickly.

The aim of this work is to test the findings of (Kotecha et al. 2022) and elucidate the mechanisms that do or do not influence the evolution of galaxies near filaments within clusters. To accomplish this, we study the distribution of galaxies undergoing RPS in filaments around clusters, using morphological classifications of galaxies from the citizen science project, "Fishing for jellyfish galaxies" in clusters Abell 85, Abell 1644, and the Shapley Supercluster region.

Based on the voting data from the public, we devised criteria to identify galaxies showcasing characteristics indicative of hydrodynamical effects in addition to measure the distance of the RPS candidates to their nearest filament.

Chapter 2

Methods

2.1 Data

The parent dataset utilized through this work is composed of optical imaging data from the *Legacy Survey DR10*[1] (LS DR10), which offers photometry in *(g,r,i,z)* bands and RGB images of the galaxies.

The study focuses on 3 areas in the following clusters:

- A85 is a massive cluster with an R_{200} of 1.29 [Mpc]. The data extends out to roughly 2.5 times R_{200}, corresponding to a distance of 238.2 [Mpc] at the cluster's redshift, $z = 0.055061$.
- A1644 is a massive cluster with an R_{200} of 1.20 [Mpc]. The data extends to approximately 2.5 times R_{200}, which corresponds to a distance of 199.4 [Mpc] at the cluster's redshift, $z = 0.047399$.
- We cover a large region of the Shapley Supercluster, which spans approximately 14 degrees in RA and 8 degrees in DEC, roughly corresponding to 46.5 x 26.5 [Mpc].

2.1.1 Galaxy classifications

Morphological classification of galaxies based on LS DR10 has been extracted from the citizen science project, Fishing for Jellyfish Galaxies[2], hosted on Zooniverse[3]—a website that enables volunteers to participate in various research projects across multiple scientific disciplines. The effectiveness of exploiting citizen scientists to sort through vast amounts of data has already been successfully demonstrated in the Galaxy Zoo project (Lintott et al. 2008; Lintott et al. 2011; Willett et al. 2013). In the Fishing for JF Galaxies project, 82 galaxy clusters have been analyzed. Inside each cluster, galaxies located within the confines of $\sim 2.5\ R_{200}$ were selected and thereafter scrutinized by 10 citizen scientists. The objective of this particular project is to gather a large catalog of Jellyfish galaxy candidates by realizing a series of visual inspection questions related to galaxy morphology in order to identify, primarily, galaxies undergoing ram-pressure stripping.

[1] Legacy Survey DR10.
[2] Fishing for Jellyfish Galaxies.
[3] Zooniverse.

To optimize the discovery of new jellyfish galaxies, the designers of the Zooniverse project "Fishing for Jellyfish Galaxies" selected spiral galaxies near galaxy cluster centers, excluding low-quality images or those too small to discern clearly (Bellhouse et al. in prep). From this reduced catalog they have taken the brightest 10,000 objects to produce the sample for this project by setting a magnitude cutoff in R at 19 mag.

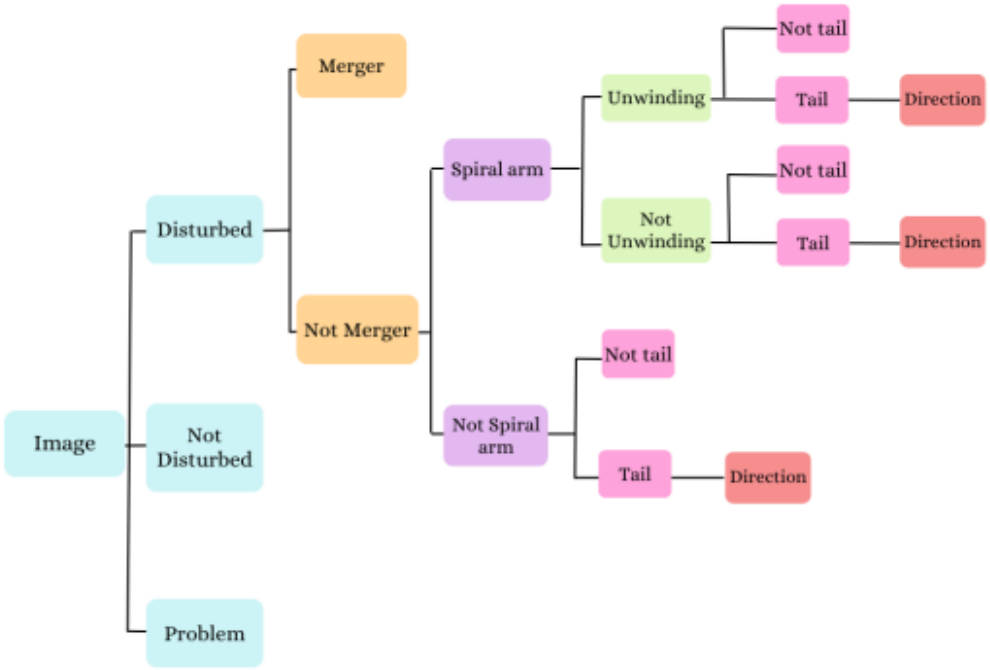

Figure 2.1: Flowchart of votes in the Fishing for Jellyfish Galaxies project. Image credit: Carolina Dulcien.

The volunteers follows the flowchart shown in Figure 2.1 as they go through the questions. Each box in the flowchart represents a question. For example, the "Disturbed" box corresponds to the question *Does the galaxy appear to be disturbed and/or asymmetric, in either the close image or the wide image?* and so forth. The break in the continuity of the flowchart signifies the conclusion of the survey. It should be noted from the flowchart that the total number of votes is the sum of *Disturbed*, *Undisturbed*, & *Problem votes*.

2.1.2 Large-scale structure

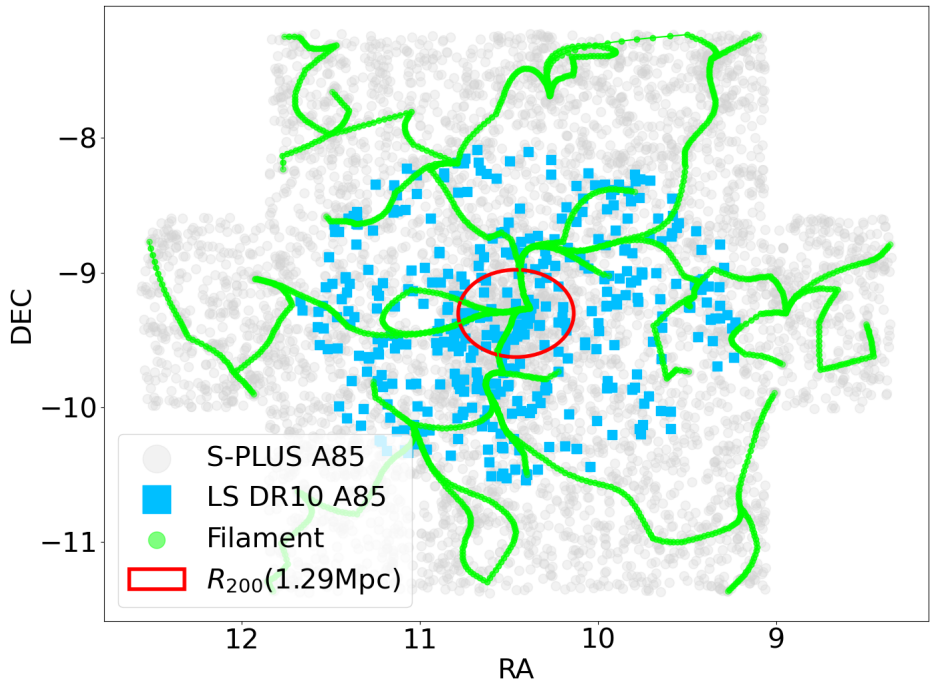

Figure 2.2: Spatial distribution of galaxies within the Abell 85 cluster, with photometric members marked in light grey and LS DR10 galaxies highlighted in cyan. The green lines represent the identified cosmic filaments, highlighting the large-scale structure within the cluster. The red circle centered at the brightest cluster galaxy (BCG), Holm 15A (10.460294, -9.303129), indicates the virial radius of 1.29 Mpc

In this pilot study, filaments were identified using *DisPERSE*[4], a software tool designed to extract and quantify the filamentary structures of the cosmic web in both 2D and 3D datasets. We use cluster member catalogues built using photometric information from LS DR10 and S-PLUS[5] multi-band photometry (Mendez et al. in preparation) to extract the filamentary structure in 2 galaxy clusters (A85 and A1644) out to $\sim 2\times$ the virial radii, and the large region enclosing the Shapley supercluster (Baier et al. in preparation).

Figure 2.2 shows the distribution in the sky of the galaxies in A85 in addition with the filaments. Light gray dots are photometrically selected cluster galaxies. Not all of these galaxies have not been used to perform the morphological analysis, they are only incorporated to visually depict the overall large-scale structure of the cluster such as the filaments which correspond to the green

[4]DisPERSE: a tool for automatic identification of persistent structures for cosmological applications

[5]S-PLUS (Southern Photometric Local Universe Survey): a survey dedicated to map the southern sky using a unique set of 12 optical filters. These filters include the five broad-band filters used by the Sloan Digital Sky Survey (SDSS) and seven narrow-band filters, designed to capture specific spectral features.

structure. On the other hand, cyan galaxies are those from the LS DR10 catalog and will be used for the morphological analysis.

2.2 Preliminary Classification Criteria

In the Zooniverse project "Fishing for JF galaxies project" each galaxy has 10 votes from 10 different classifiers. We thus needed to combine the votes to decide when a galaxy could be categorized as being affected by RPS or e.g. a merger. The following sections explain this process.

2.2.1 Vote Fractions

In total, we have 10 classifications per galaxy in the vast majority of cases, and 11 classifications in some cases, for a total of 49,703 galaxies in 82 clusters and the Shapley Supercluster region. In Table 2.1 displays three example galaxies with the corresponding vote distribution.

Cluster	ID	Disturbed	Undisturbed	Problem	Merger	Unwinding	Tail
A85	99066	5	4	1	0	0	5
A1644	99067	3	6	2	1	0	4
Shapley	99068	4	5	1	0	2	3

Table 2.1: Number of votes for each galaxy state: disturbed, undisturbed, problem, merger, unwinding, and tail.

To facilitate a more straightforward comparison and analysis of the vote distribution, we calculate vote fractions. These fractions, computed for the various classes outlined in the flowchart of Figure 2.1, serve not only to summarize the voting patterns but also to establish criteria for categorizing galaxies. For example, a disturbed vote fraction is defined as:

$$F_{\text{dist}} = \frac{\text{Disturbed votes}}{\text{Disturbed votes} + \text{Undisturbed votes}} \tag{2.1}$$

and represents the number of voters that thought the galaxy was disturbed.

Likewise, merger fraction is defined as:

$$F_{\text{mer}} = \frac{\text{Merger votes}}{\text{Disturbed votes}} \tag{2.2}$$

Tail fraction is defined as:

$$F_{\text{tail}} = \frac{\text{Tail votes}}{\text{Not Merger votes}} \tag{2.3}$$

Problem votes was not considered when creating the fractions because most of the galaxies cataloged as problems by the citizen scientists were not actually problematic. It is important to remark that we did not possess the votes for 'Spiral Arm' or 'Not Spiral Arm', meaning they were also not considered when creating the vote fractions. The aim of these vote fractions is to aid in defining clear criteria for distinguishing between Jellyfish candidates and Unwinding candidates.

With this in mind, we now formally define the non-merger fraction:

$$F_{\text{notmerg}} = \frac{\text{Tail votes + No Tail votes}}{\text{Disturbed votes}} \tag{2.4}$$

In Table 2.2 we can appreciate the different vote fractions for the example galaxies from Table 2.1:

Cluster	ID	F_{dist}	F_{mer}	F_{tail}	F_{notmerg}
A85	99066	$\frac{5}{9}$	0	$\frac{5}{5}$	$\frac{5}{5}$
A1644	99067	$\frac{3}{9}$	$\frac{1}{3}$	$\frac{5}{9}$	$\frac{2}{3}$
Shapley	99068	$\frac{4}{9}$	0	$\frac{3}{4}$	$\frac{4}{4}$

Table 2.2: Vote fractions for the example galaxies

2.2.2 Validation of public votes

To be able to use the vote fractions to identify galaxies undergoing RPS we first validate our public votes against the largest sample of known RPS candidates from the literature. These samples consist of hundreds of galaxies extracted from the work of Poggianti et al. 2016 and Vulcani et al. 2022.

Poggianti et al. 2016 conducted a systematic search for jellyfish galaxy candidates at low redshift, utilizing data from the WINGS (WIde-field Nearby Galaxy-cluster Survey) and OmegaWINGS surveys. They identified a sample of 344 jellyfish galaxy candidates out of 70 galaxy clusters. These galaxies exhibit clear signs of ram pressure stripping, such as extended tails of stripped gas and star formation regions. The galaxies were classified using a JClass system, where galaxies are assigned a grade from JClass 1 to JClass 5 based on the intensity and clarity of the stripping features, with JClass 5 representing the most prominent examples.

Vulcani et al. 2022 focused on the relevance of ram pressure stripping for the evolution of blue cluster galaxies at optical wavelengths. The authors analyze the proportion of galaxies exhibiting signs of stripping at optical wavelengths using data from 66 clusters included in the WINGS and OMEGAWINGS surveys. Their study concentrates on the infalling galaxy population, specifically those that are blue, bright ($B < 18.2$), late-type, and confirmed as cluster members through spectroscopy, located within two virial radii. In addition to the "traditional" stripping candidates (SC), which display unilateral debris and tails, they also include unwinding galaxies (UG) as potential stripping cases, which are spiral arms that appear stretched out and distorted due to the stripping forces. SC and UG each represent approximately 15%–20% of the inspected sample. If we assume that both types are undergoing ram pressure stripping, we can conclude that about 35% of the infalling cluster population shows signs of stripping in their morphology at optical wavelengths in the low-z universe. The galaxies in this study were categorized using a UClass system, which grades the galaxies based on the prominence of the unwound spiral arms (from 1 to 5), with UClass 5 representing the most significant examples of unwound arms.

We will refer to the catalogs generated by these two studies as Jellyfish galaxies, which we will term the literature JF sample, focusing specifically on those with $JClass \geq 3$. To validate the

distribution of public votes on these galaxies, we will verify the correlation between public votes and established findings from Poggianti et al. 2016 and Vulcani et al. 2022. These public vote distributions are illustrated in Figure 2.3 and Figure 2.4, respectively.

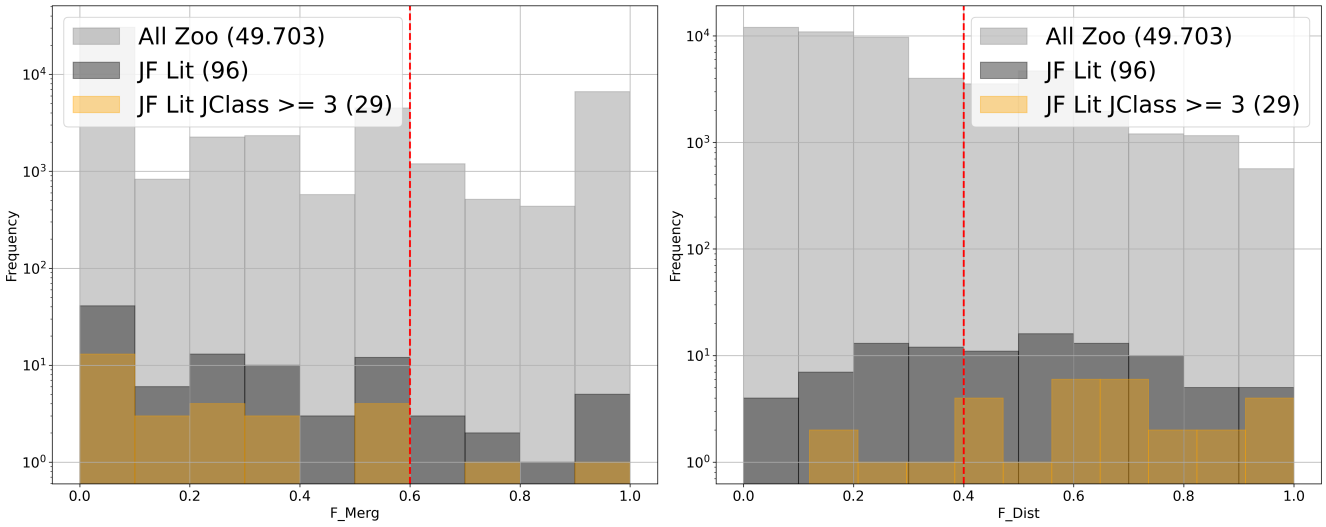

Figure 2.3: Distribution of votes on the Stripping Candidates from Poggianti and Vulcani's research, based on Zooniverse data. The left histogram shows the F_{mer} distribution, and the right shows the F_{dist} distribution. Categories: All Zoo (49,703), JF Lit (96), and JF Lit JClass ≥ 3 (29). The y-axis is on a logarithmic scale.

Figure 2.3 illustrates the distribution of "merger" and "disturbed" votes made by citizen scientists across three samples. The light gray distribution represents the 49,703 galaxies in the "Fishing for Jellyfish Galaxies" project. The dark gray distribution corresponds to the 96 jellyfish galaxies identified in the literature (Poggianti+Vulcani catalog), while the dark yellow distribution represents the 29 jellyfish galaxies with JClass ≥ 3. From the latter distribution, is deductible that citizen scientists observed few merger features and several perturbation features in jellyfish galaxies with JClass ≥ 3. This suggests that the citizen scientists agreed with researchers on the most prominent examples from the literature, validating citizen science as an effective tool for such studies.

Based on this exercise alone, one could propose a preliminary criteria to select real JF candidates from the citizens' votes. For example, in Figure 2.3 the cuts $F_{\text{mer}} \leq 0.6$ and $F_{\text{dist}} \geq 0.4$ contain most of the confident JF candidates from the literature.

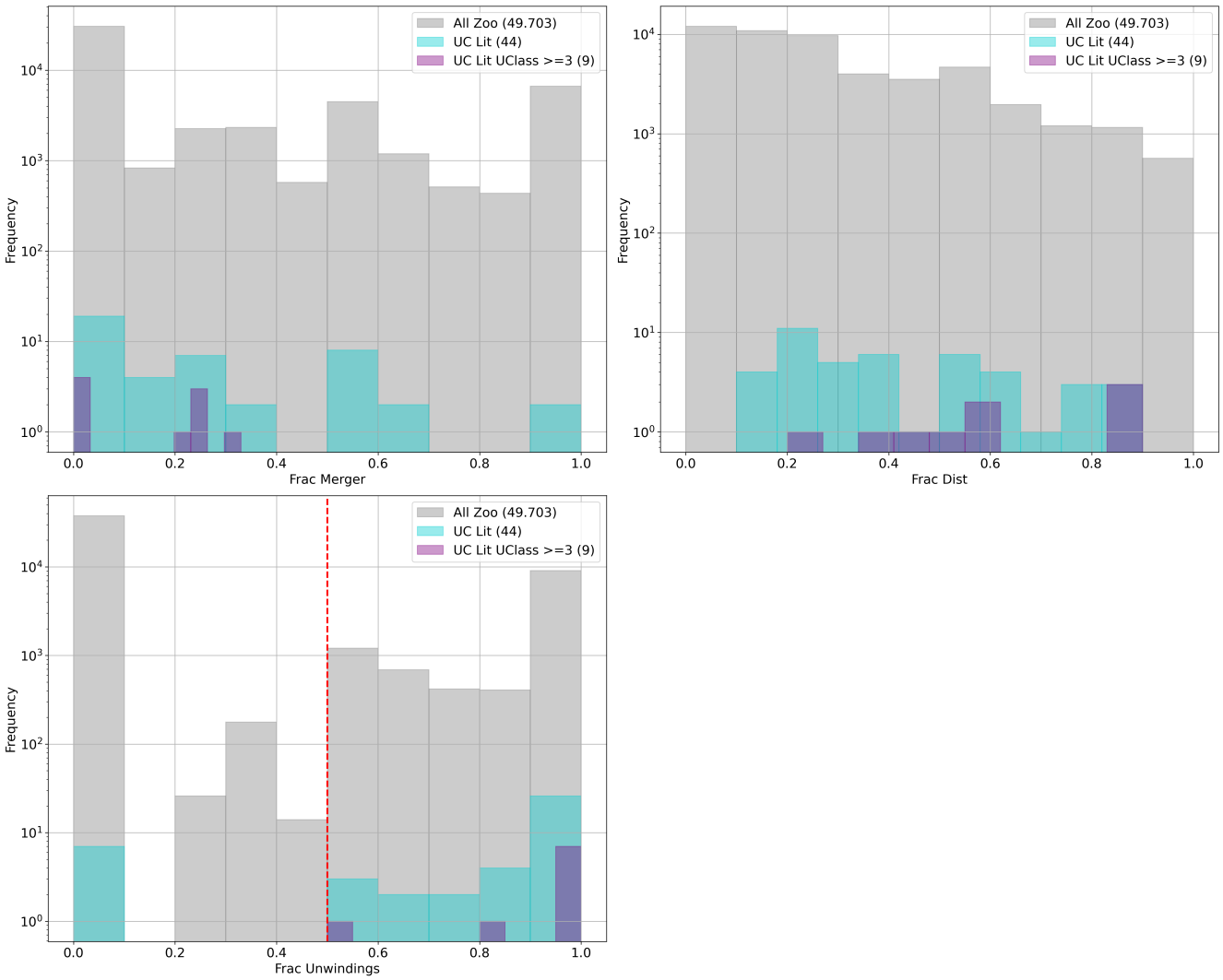

Figure 2.4: Distribution of votes on the Unwinding Candidates from Vulcani's research, based on Zooniverse data. Similar to the previous figure, the only additional distribution is for F_{unw}. Categories: All Zoo (49,703), UC Lit (44), and UC Lit UClass ≥ 3 (9).

In Figure 2.4 we now plot the unwinding galaxy candidates from the literature. The light gray distribution is the same as in Figure 2.3, the cyan distribution corresponds to the 44 unwinding galaxies identified in the literature (Vulcani's catalog), and the purple distribution represents the 9 unwinding galaxies with UClass ≥ 3. Although the last distribution contains relatively few galaxies, there is a discernible trend where citizen scientists tend to vote for fewer merger features and a majority of disturbed and unwinding features. This trend aligns with Vulcani's research, enhancing the reliability of citizen scientists in identifying these features.

Based on Figure 2.4, a possible threshold to selecting UG candidates using public votes could be:

$$F_{\text{unw}} \geq 0.5 \tag{2.5}$$

2.3 Criteria to select disturbed galaxies

To select the best criteria to construct a complete and pure JF candidate sample, a Monte Carlo analysis[6] was conducted.

To quantify the purity and completeness of galaxy samples from the Zooniverse project, it is essential to have a sub-sample of galaxies with a "true" classification. This reference sample was assembled by experts in the field[7], who focused on visually identifying hydrodynamical and gravitational effects, specifically RPS and mergers, for each galaxy in A1644. Our research will concentrate solely on the RPS candidates. The experts assigned a confidence value from 1 to 3, with 3 being the highest. Only galaxies with confidence values of 2 or higher were included in this subset, ensuring the inclusion of promising RPS candidates.

The concepts of purity and completeness arise from the need to quantify the accuracy of public voting. To achieve this, we must apply specific criteria to the 403 galaxies within A1644 in the Fishing for Jellyfish Galaxies project. A criteria is defined as a set of conditions based on voting fractions. The galaxies that remain after applying these criteria constitute the citizen science-selected sample. To quantify the alignment between the citizen science-selected sample and the expert sample, we define two metrics: purity (ρ) and completeness (ζ). These metrics are formally expressed in Equation 2.6 and Equation 2.7, respectively and can be computed after applying any criteria.

Purity is the ratio of the number of galaxies in the citizen science-selected sample that also belong to the expert sample, to the total number of galaxies in the citizen science-selected sample. This ratio addresses the question: "How many expert-classified candidates are in the citizen science-selected sample?".

$$\rho = \frac{\text{N° galaxies from the citizen science-selected sample within the expert sample}}{\text{N° galaxies from the citizen science-selected sample}} \tag{2.6}$$

Completeness is the ratio of the number of galaxies in the citizen science-selected sample that also belong to the expert sample, to the total number of galaxies in the expert sample. This ratio addresses the question: 'How many expert-classified candidates are we not considering in citizen science selected sample?'.

$$\zeta = \frac{\text{N° galaxies from the citizen science-selected sample within the expert sample}}{\text{N° galaxies from the expert JF sample}} \tag{2.7}$$

Both metrics take values between 0 and 1. A purity value closer to 1 indicates that the citizen science-selected sample is predominantly composed of prominent RPS candidates, while a value closer to 0 suggests that most of the citizen science RPS candidates are not prominent examples. Similarly, a completeness value near 1 implies that most RPS candidates, both prominent and not, are included in the sample, though it may also contain many false positives. In contrast, a completeness value near 0 indicates that very few of the RPS candidates are captured in the sample.

[6]Developed by Ignacio Quiroz and Carolina Dulcien.

[7]Carolina Dulcien, Yara Jaffé and Jacob Crossett

Figure 3.1 graphically illustrates the definitions of purity and completeness in the citizen science-selected sample, which will be explained in detail later.

In A1644, a Monte Carlo analysis was conducted to test multiple values for a certain criteria aiming to maximize both completeness and purity. This criteria is shown in Equation 2.8, where X, Y, and Z are the values that will be systematically varied to seek optimization. Each combination generates a different sample of JF candidates with distinct values of purity and completeness. This approach aims to identify the criteria that best captures the maximum number of JF galaxies in A1644. By systematically varying these values, the analysis seeks to ensure that the selected sample contains the most representative and accurate JF galaxies in A1644, enhancing the reliability of the study.

$$F_{\text{dist}} \geq X \quad \& \quad (F_{\text{tail}} \geq Y \quad \text{or} \quad F_{\text{notmerg}} \geq Z) \tag{2.8}$$

Figure 2.5, shown below, displays the overall results from the Monte Carlo analysis applied in A1644. The color bar indicates the purity (left panel) and completeness (right panel) of the sample based on different values of the vote fractions. It is evident from the figure that purity and completeness are inversely proportional. To maximize both, we should select criteria near the middle of Figure 2.5, where purity and completeness can achieve their maximum values simultaneously.

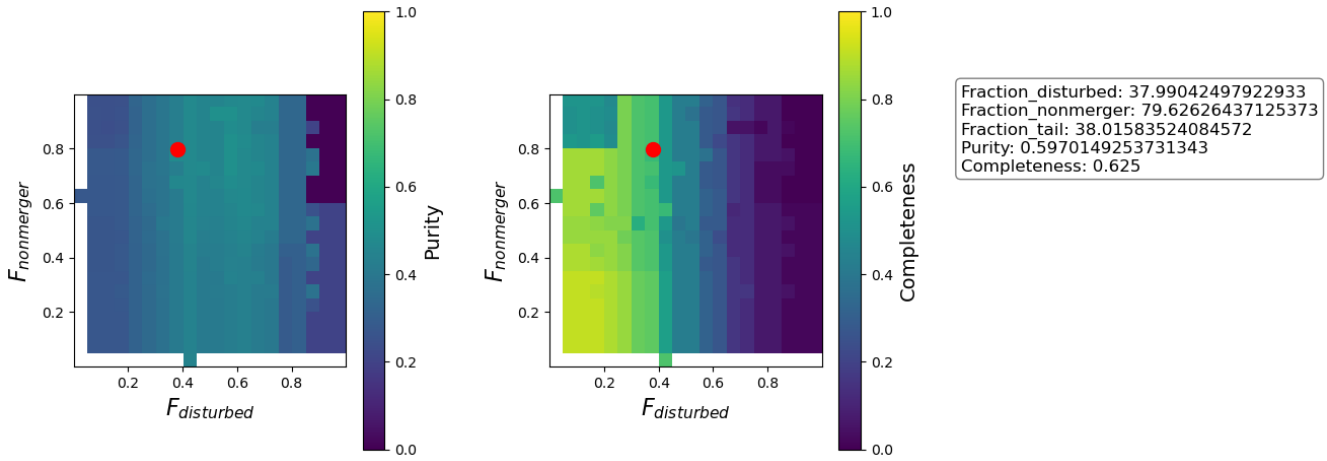

Figure 2.5: Results from the Monte Carlo analysis applied to A1644, illustrating how different values of the vote fractions affect the purity (left panel) and completeness (right panel) of the sample. The color bar indicates the degree of purity and completeness, with the middle region suggesting an optimal balance between the two metrics.

After running the Monte Carlo analysis, we selected the criteria that maximize both purity and completeness in A1644. The objective is to apply these optimized criteria not only to A1644 but also to A85 and the Shapley supercluster region. The selected criteria is shown in Equation 2.9.

$$F_{\text{dist}} \geq 0.36 \quad \& \quad (F_{\text{tail}} \geq 0.38 \quad \text{or} \quad F_{\text{notmerg}} \geq 0.79) \tag{2.9}$$

The intersection of the vote fractions values, as well as the pixel-color, are highlighted with red lines in Figure 2.5. Specifically, the purity for these criteria is ~ 0.59, and the completeness is ~ 0.62. This set of conditions on the vote fractions displayed in Equation 2.9 will be applied to A85

and the Shapley supercluster region in order to find new JF candidates.

2.4 Distance to the nearest filament

We aim to measure the distance between RPS candidate galaxies and their nearest filamentary structures to investigate a possible correlation between the RPS phenomenon and these large-scale cosmic filaments. To achieve this, a code[8] was developed that calculates the shortest distance from a point (representing a galaxy) to a line segment (representing a segment of a filament).

In this context, filaments are two-dimensional structures generated by the *DisPERSE* algorithm and consist of multiple segments. The code uses cosmological parameters to convert angular distances in the sky into physical distances, using the redshift of the galaxy cluster for accuracy. Specifically, the code identifies the closest line segment from an array of segments representing filaments to a given galaxy's position (specified in right ascension and declination).

By calculating distances in both degrees and megaparsecs, this tool effectively maps and analyzes the large-scale structures of galaxy clusters. The result is a powerful method for examining the spatial relationships between RPS galaxies and cosmic filaments, potentially uncovering insights into the environmental factors influencing galaxy evolution.

[8]Provided by Lawrence Bilton.

Chapter 3

Results

3.1 Candidates

The number of jellyfish galaxies and unwinding galaxies remaining after applying Equations 2.9 and 2.5, respectively, to the LS DR10 datasets of A1644, A85, and the Shapley supercluster region are displayed in Table 3.1. The table also shows the fractions of these galaxies relative to the total number of galaxies in the Fishing for Jellyfish project for each cluster.

Cluster	No. Zoo galaxies	No. JF	No. UG	F_{JF}	F_{UG}
A85	418	102	100	24.4 %	23.9 %
A1644	403	67	96	16.62 %	23.8 %
Shapley SC	8679	2104	2199	24.2 %	25.3 %

Table 3.1: Number of galaxies classified as jellyfish (JF) and undisturbed (UG) in various clusters, along with their respective fractions (F_{JF} and F_{UG}).

In contrast to the findings of Vulcani et al. 2022, who reported that 15-20% of blue spiral galaxies moving towards the centers of clusters undergo ram pressure stripping based on a large sample from the WINGS/OmegaWINGS surveys, our study finds slightly higher percentages when we analyzed JF and UG as different samples. We observed ram pressure stripping rates between 20-25%, except for the JF candidates in the A1644 cluster, where the fraction F_{JF} falls within the range reported by Vulcani et al. 2022. This suggests that a higher proportion of blue spiral galaxies moving towards cluster centers may be undergoing ram pressure stripping than previously reported.

When we consider both JF and UG as features of galaxies undergoing ram-pressure stripping, our results align more closely with those of Vulcani et al. 2022. To achieve this, we combine the samples of JF and UG candidates and subtract the galaxies that belong to both samples. The proportion of these galaxies relative to the total within each cluster reveals that in A85, 35.41% of the blue galaxies exhibit features of ram-pressure stripping in the optical. In A1644, the percentage is 30.27%, and in the Shapley supercluster region, it is 38.10%.

We can now show the purity and completeness of our JF candidate sample in A1644. Figure 3.1 illustrates the concepts of purity and completeness for the JF candidate sample that we generate

using the MC analysis criteria. Note that this analysis cannot be applied to the UG candidates, as there is no expert sample of UG galaxies in A1644.

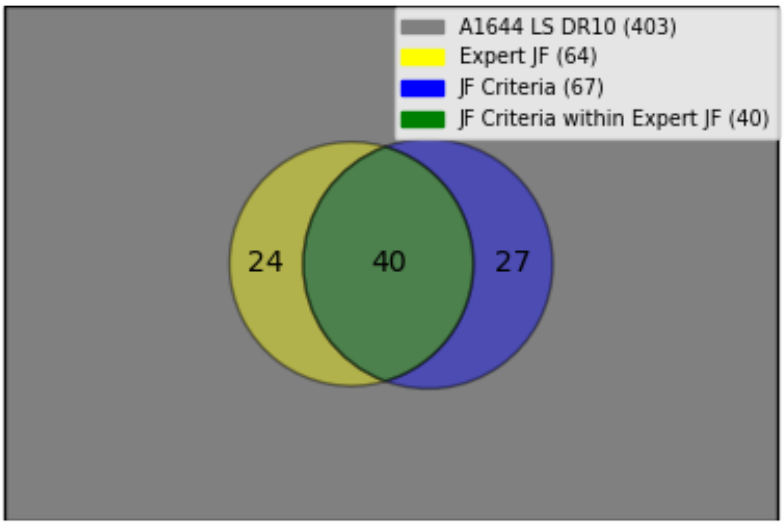

Figure 3.1: Venn diagram of the samples in A1644. Yellow set is the expert JF sample (64), the blue set is the JF candidates sample (67) from the MC criteria and the green overlap indicates the galaxies that belong to both sets (41).

Figure 3.1 shows that the JF candidate sample generated through the MC analysis criteria has significant overlap with the expert sample of JF galaxies in A1644, indicating high purity. At the same time, this sample encompasses more than half of the JF galaxies in A1644.

To compute the purity, we use Equation 2.6, which gives us a result of $\frac{40}{67} = 0.5970$. In contrast, Equation 2.7 provides the completeness, calculated as $\frac{40}{64} = 0.625$

In Figure 3.2, we observe different candidates: the first row displays the JF candidates, while the second row shows some of the UG candidates. Both rows are ordered from left to right as A85, 1644, and Shapley.

Figure 3.2: Mosaic of astronomical candidates. The first row displays images of Jellyfish (JF) galaxy candidates, showcasing distinctive features such as tidal tails and asymmetrical structures. The second row presents a selection of unwinding galaxy (UG) candidates, characterized by their unique spiral structures and unwinding arms.

In general, JF candidates demonstrate perturbations on the disk along with subtle features of tails, leading to asymmetries. In contrast, UG candidates are spiral galaxies with prominent arms that appear to be loosening or spreading out.

3.2 Location of jellyfish and unwinding galaxies with respect to the cosmic web

In this section, we aim to test the hypothesis proposed by Kotecha et al. 2022, which suggests that ram pressure stripping decreases near intracluster filaments but increases in the outskirts. The Zooniverse candidates cover a wider region than previous systematic searches for jellyfish galaxies, making them a valuable alternative for testing Kotecha et al. 2022's findings across several clusters. We will analyze and compare the distance distributions of galaxies to their nearest filament in two main samples: the JF & UG galaxy candidates and all galaxies identified in the Zooniverse project for each cluster. We will apply two statistical tests, the Kolmogorov-Smirnov (K-S) test and the Anderson-Darling (A-D) test, to determine whether there is a significant difference between these distributions. These tests will allow us to assess whether the spatial distribution of jellyfish galaxies supports the proposed hypothesis regarding the influence of intracluster filaments on ram pressure

stripping.

In first instance we visually assess the locations of the candidates relative to the filaments, we have plotted the sky distribution of JF and UG candidates for all clusters in the study. Top panels from Figures 3.3 to 3.5 displays the sky distribution of multiple samples: cyan stars represent JF candidates, fuchsia triangles indicate UG candidates, light gray circles denote photometric members (from S-PLUS), and dark gray circles represent the Zooniverse galaxies (LS DR10). Figures 3.3 and 3.4 also include UG literature galaxies (blue squares) and JF literature galaxies (black circles). Neither Poggianti et al. 2016 nor Vulcani et al. 2022 searched for JF galaxies in the Shapley supercluster region, which is why there are none in Figure 3.5. Additionally, photometric cluster members are not shown because we did not posses the dataset for the Shapley supercluster. In all clusters studied, some JF candidates are also categorized as UG candidates, and are referred to as common candidates.

The bottom panels from Figures 3.3 to 3.5 shows histograms that compares the distributions of the nearest distances to the filament for both the candidate galaxies and the Zooniverse galaxies in A85, A1644 and Shapley, respectively. As in the top panel, the colors represent the same samples. The only addition is the green distribution, which corresponds to the common candidates. We performed both a K-S test and an A-D test between each candidates distribution and the Zooniverse galaxies distribution.

The K-S test is a non-parametric test that compares the cumulative distribution functions (CDFs) of two datasets to assess whether they come from the same distribution. The A-D test is a modification of the K-S test that gives more weight to the tails of the distribution. Both of these tests are used for hypothesis testing, where the null hypothesis is that both samples are drawn from the same continuous distribution. The tests rely on the significance level (p-value), which corresponds to the probability of observing a test statistic as extreme as, or more extreme than, the one calculated from the data, given that the null hypothesis is true. A small p-value, typically less than 0.05, indicates there is less than a 5% chance of obtaining a K-S or A-D statistic as large as the one observed if the two samples were indeed from the same distribution, leading to the conclusion that the distributions are likely different. A high p-value indicates that the observed statistic is not extreme. It is consistent with what we would expect if the null hypothesis were true, thus supporting the null hypothesis.

The K-S statistic corresponds to the maximum deviation between the CDFs of the two distributions. A larger K-S statistic indicates a greater difference between the distributions. Meanwhile, the A-D statistic reflects how well the empirical CDF of one sample matches the other, with higher values indicating a poorer fit. Both statistics help determine whether the differences between distributions are significant.

Top panel of Figure 3.3 shows that neither the MC criteria nor the criteria for UG candidates were able to encompass all the galaxies from the literature. However, they do encompass the vast majority of them (5 out of 6), suggesting that while both criteria are effective for selecting candidates, they could still be refined. In addition, it is evident that multiple JF candidates are also UG candidates. Although these galaxies are not explicitly highlighted, those that share common coordinates in both samples are the previously mentioned common candidates.

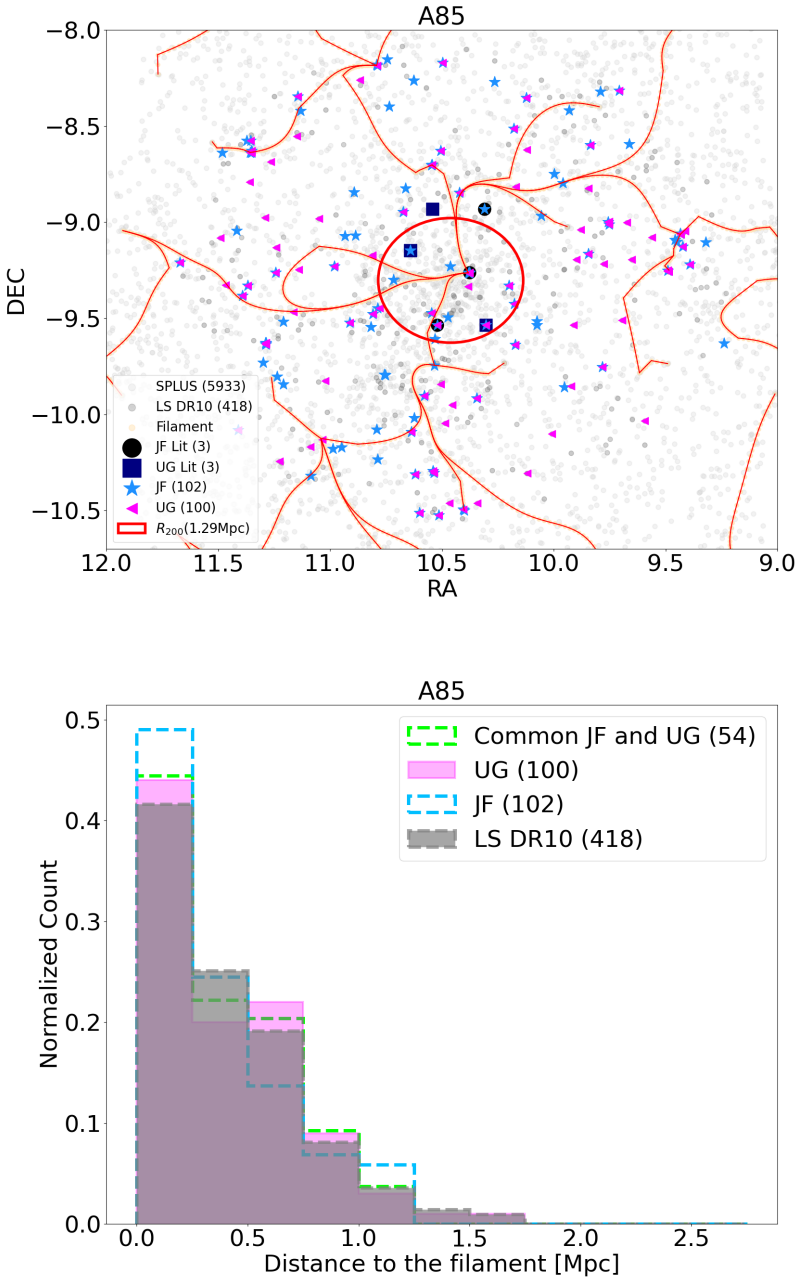

Figure 3.3: Top: Sky distribution of galaxies in A85. Photometric cluster members are shown in light gray Zooniverse-classified galaxies in dark gray, known Jellyfish and Unwinding galaxies from the literature in black circles and blue squares respectively. Additionally, selected JF galaxies identified through MC criteria (cyan stars), Unwindings candidates (fuchsia triangles) and common candidates are plotted, along with filament structures. Bottom: Distribution of distances from A85 galaxies to their nearest filament.

Preliminary, from the lower panel of Figure 3.3 we the distribution of JF candidates seems to show a slight clustering at low distances with respect to the Zooniverse galaxies distribution. To

quantify the difference, the statistical tests have been performed between each candidate sample and the Zooniverse sample.

A85				
	KS		AD	
Sample	**p-value**	**Statistic**	**p-value**	**Statistic**
JF	0.0858	0.547	0.143	0.877
UG	0.284	0.108	0.25	0.103
Common	0.228	0.147	0.219	0.439

Table 3.2: Results from statistical tests (K-S & A-D) applied in A85.

Table 3.2 shows the significance level and the statistic value of each statistical test applied to the distributions in Abell 85. Based on the p-values of both tests, we affirm that there is insufficient evidence to claim that there is a significant difference between the distributions. This indicates that the distances to the filament for both groups (any candidate sample and the Zooniverse sample) are similar. As a result, there is no significant evidence to suggest that candidates prefer different proximities to filaments compared to other galaxies within A85.

Top panel of Figure 3.4 shows that the criteria did not capture the majority of the JF galaxies from the literature within A1644; in this case, only 3 out of 9 JF galaxies were identified. This implies that the criteria need refinement. In a manner similar to the previous figure, multiple candidates share coordinates in both samples.

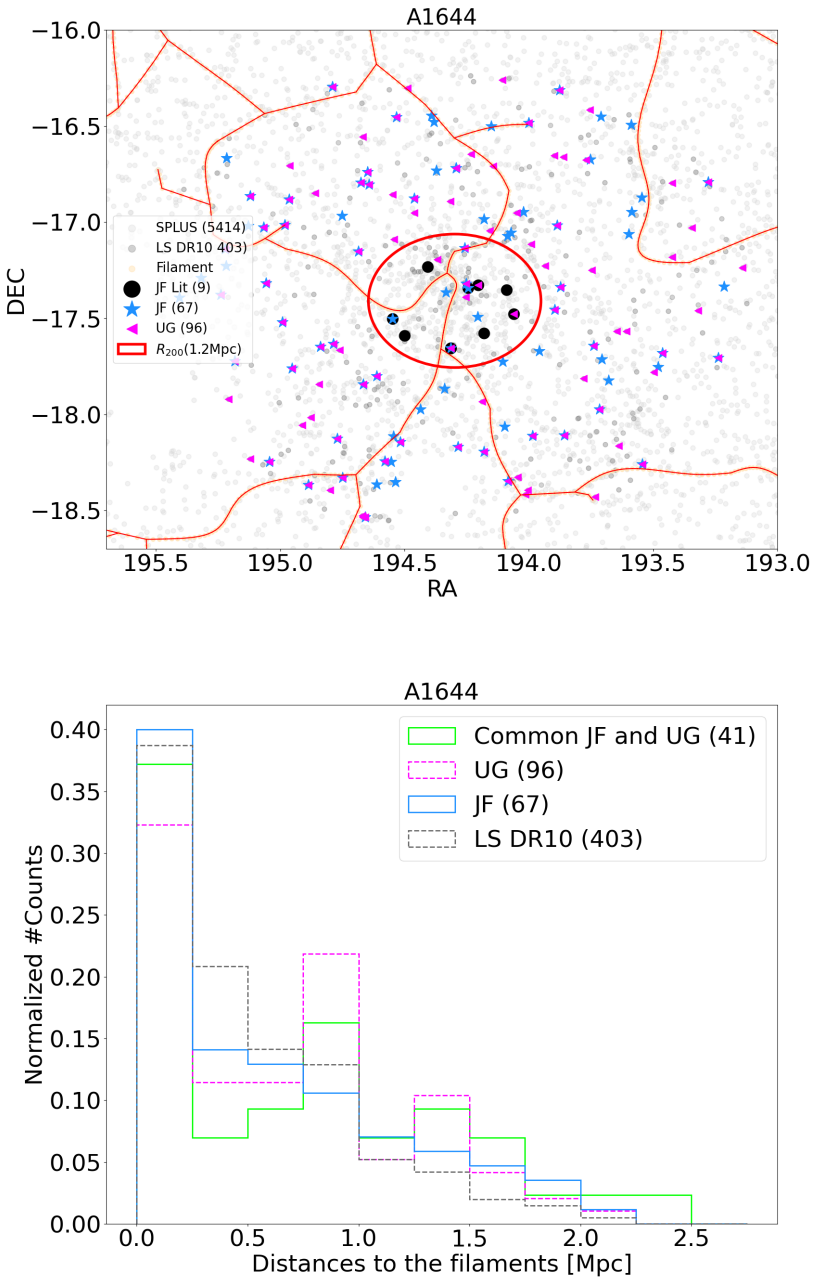

Figure 3.4: Top: Spatial distribution of A1644. Likewise in the previous Figure same samples are used. Bottom: Distribution of distances from A1644 galaxies to their nearest filament.

In contrast to the bottom panel of the preceding Figure, the bottom panel of Figure 3.4 shows little difference between the distributions in this histogram. The main difference arises from the UG distribution, where we observe some clumps of UG candidates between ∼1 and 1.5 R_{200}. However, these clumps are not present in either the JF or common candidates distributions, indicating that they do not have much weight on the overall.

Table 3.3 exhibits the p-values alongside the statistics value from each test applied to the

distribution in Figure 3.4

A1644				
	KS		AD	
Sample	**p-value**	**Statistic**	**p-value**	**Statistic**
JF	0.419	0.103	0.25	0.265
UG	0.00493	0.194	0.00512	4.533
Common	0.0271	0.230	0.0117	3.57

Table 3.3: Results from statistical tests (K-S & A-D) applied in A1644.

Based on the statistical results, we observe that the UG distribution exhibits low p-values in both the KS and AD tests, indicating a significant difference from the Zooniverse distribution. This suggests that UG candidates prefer different proximities to filaments compared to other galaxies within the cluster. Furthermore, the significant difference is also evident in the common candidates, as indicated by their low p-values. This finding contrasts with previous clusters, where such differences were not observed. Therefore, in the A1644 cluster, there is substantial evidence to suggest that certain galaxy candidates are distributed differently in relation to filaments.

Top panel of Figure 3.5 shows the multiple JF and UG candidates that have been found in the Shapley supercluster region. Without any preference, galaxies are widely distributed along this region. Several common candidates can be identified on the first look.

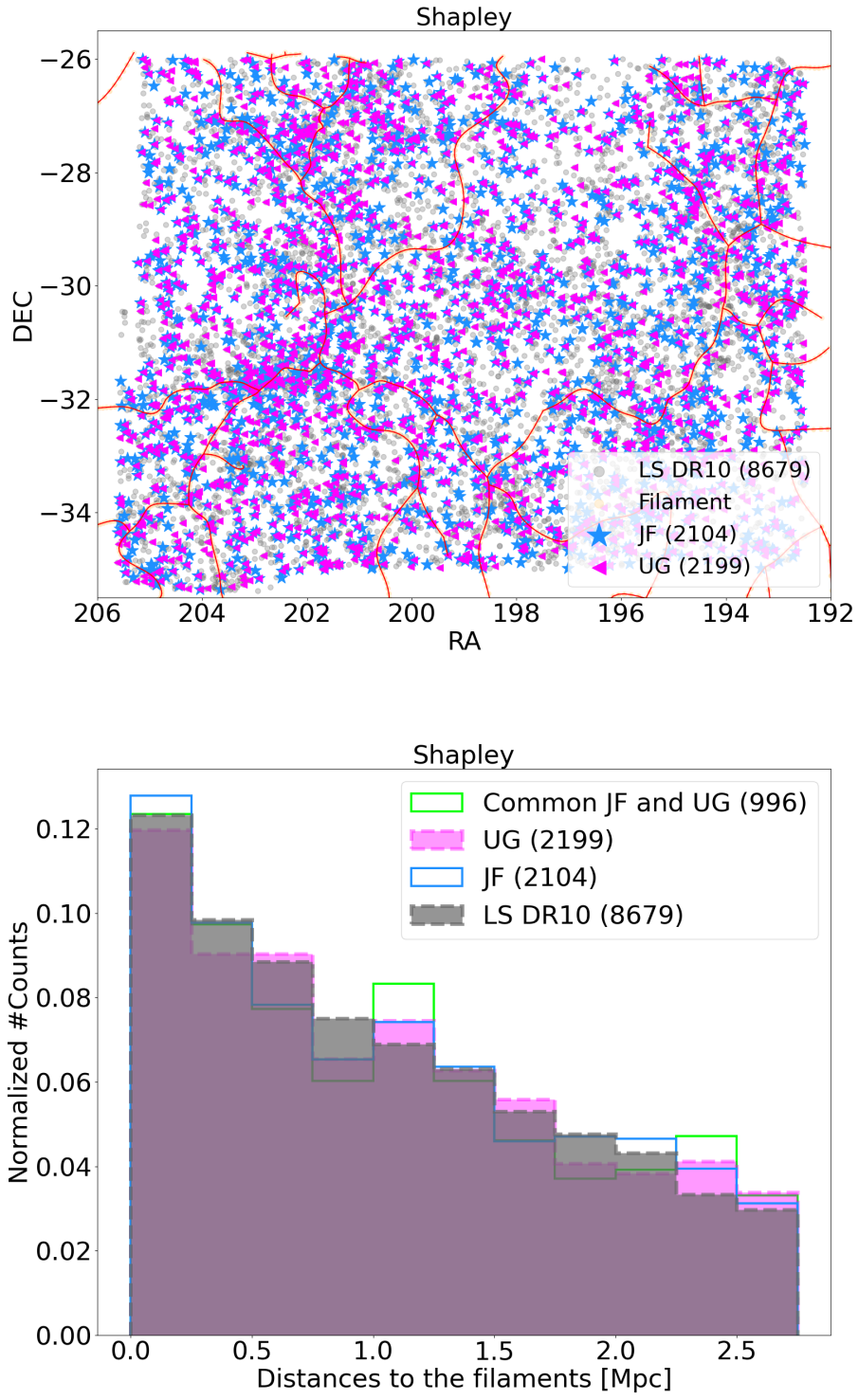

Figure 3.5: Top: Spatial distribution of Shapley. Likewise in the previous Figure same samples are used. Bottom: Distribution of distances from Shapley galaxies to their nearest filament.

Bottom panel shows a null difference between distribution at first glance. All of the distribution

are really alike on this region. Signifying that there is no preference on were the candidates can be found. Leading to suggest that similar to the previous clusters, there is no significant evidence to suggest that candidates in Shapely prefer different proximities to filaments compared to other galaxies. This is supported with the p-values that are presented in Table 3.4

Shapley				
	KS		**AD**	
Sample	**p-value**	**Statistic**	**p-value**	**Statistic**
JF	0.419	0.103	0.25	0.265
UG	0.376	0.0241	0.25	0.151
Common	0.169	0.0374	0.175	0.662

Table 3.4: Results from statistical tests (K-S & A-D) applied in Shapley.

In summary, our analysis of the spatial distributions of JF and UG galaxy candidates relative to cosmic filaments across the clusters A85, A1644, and Shapley reveals no substantial differences between these candidates and the broader Zooniverse galaxy sample. The K-S and A-D test results show that the distances from the nearest filament for JF and UG candidates are statistically similar to those of the general galaxy populations in each cluster, with the exception of some minor differences observed in the UG distribution within A1644. This suggests that, in general, neither JF nor UG candidates show a significant preference for proximity to filaments compared to other galaxies in these clusters. However, it is important to note that these results are based on only three out of the 82 clusters studied, which limits the statistical robustness of our findings. To draw more definitive conclusions regarding the influence of filament proximity on galaxy types, a broader sample including more clusters is necessary. The quantified similarities between the distributions imply that ram pressure stripping or unwinding effects do not exhibit a distinct dependence on filament proximity in the studied regions, but further research with an expanded dataset is required to substantiate these results.

Chapter 4

Conclusion and future perspectives

In this preliminary investigation, we leveraged citizen science vote data from the *Fishing for Jellyfish Galaxies* project to identify candidate galaxies experiencing ram-pressure stripping (RPS), specifically Jellyfish (JF) and Unwinding (UG) galaxies. We examined their spatial distributions relative to filaments within three galaxy clusters: A85, A1644, and Shapley. To evaluate the influence of filament proximity on RPS candidates, we employed the Kolmogorov-Smirnov (K-S) test and Anderson-Darling (A-D) test to compare the distances of these candidates to the nearest filament against the distances of all other galaxies within each cluster. The objective was to assess whether these distributions differ significantly, thereby providing insights into the potential role of filaments in driving galaxy evolution. Our findings indicate that:

- In clusters A85 and A1644, not all JF or UG galaxies previously identified in the literature were captured by the citizen scientists (and filtered by our criteria). This discrepancy suggests that the citizen scientists are not always able to identify subtle RPS features and/or that the criteria used to identify these candidates may require refinement to improve the accuracy of our selection process.

- The fraction of galaxies showing RPS features is 16–25%, which is consistent with (although moderately higher than) the 15–20% reported by Vulcani et al. (2022). Specifically, our analysis reveals varying rates of RPS across different galaxy clusters. For individual samples, we observe RPS rates of 24.4% for JF candidates and 23.9% for UG candidates in A85, 16.62% for JF and 23.8% for UG in A1644, and 24.2% for JF and 25.3% for UG in the Shapley cluster. When combining JF and UG candidates, the RPS rates increase to 35.41% in A85, 30.27% in A1644, and 38.10% in the Shapley cluster. These findings suggest a potentially higher prevalence of RPS when considering both candidate samples together, indicating that combining samples can provide a more comprehensive understanding of RPS in cluster environments.

- When inspecting the spatial distribution of identified RPS and UG candidates relative to large-scale filaments, we did not find significant differences compared to the parent population of late-type galaxies. This observation, supported by the K-S and A-D tests, indicates that the spatial distributions of JF and UG candidates are statistically similar to other galaxies in the studied clusters. Consequently, proximity to filaments does not appear to be a primary driver of RPS or other hydrodynamical effects on these galaxies within the clusters.

- In the A1644 cluster, both UG and Common candidates display significant differences in distribution compared to the Zooniverse sample, as indicated by low p-values in the KS and AD tests. For UG candidates, this suggests a distinct preference for specific proximities to filaments, potentially linked to unique environmental factors or non-RPS processes. Common candidates also show notable deviations, indicating that their distribution relative to filaments differs significantly from other samples. This divergence, especially outside of filaments, could reflect underlying differences in galaxy evolution or environmental interactions. These findings highlight the need for further exploration to understand the implications of these distribution patterns fully.

Our pilot study focused on three cluster regions and found no significant preference for RPS candidates or unwinding spirals to live near or far from filaments. In fact, the spatial distribution relative to the large-scale filaments is similar to that of the parent sample of late-type galaxies. To further test the hypothesis that filaments could shield galaxies entering clusters from RPS (Kotecha et al., 2022), we need to consider, in addition to the distance from filaments, the distance from the cluster centers. In a future work we will do this, and also extend the sample to 82 other clusters with available data to have statistical robustness.

Bibliography

Boselli, A. and Gavazzi, G. (2006). Environmental Effects on Late-Type Galaxies in Nearby Clusters. , 118(842):517–559.

Cautun, M., van de Weygaert, R., Jones, B. J. T., and Frenk, C. S. (2014). Evolution of the cosmic web. , 441(4):2923–2973.

Chung, A., van Gorkom, J. H., Kenney, J. D. P., Crowl, H., and Vollmer, B. (2009). VLA Imaging of Virgo Spirals in Atomic Gas (VIVA). I. The Atlas and the H I Properties. , 138(6):1741–1816.

Cortese, L., Catinella, B., and Smith, R. (2021). The Dawes Review 9: The role of cold gas stripping on the star formation quenching of satellite galaxies. , 38:e035.

Dressler, A. (1980). Galaxy morphology in rich clusters: implications for the formation and evolution of galaxies. , 236:351–365.

Fossati, M., Fumagalli, M., Gavazzi, G., Consolandi, G., Boselli, A., Yagi, M., Sun, M., and Wilman, D. J. (2019). MUSE sneaks a peek at extreme ram-pressure stripping events - IV. Hydrodynamic and gravitational interactions in the Blue Infalling Group. , 484(2):2212–2228.

Fujita, Y. (2004). Pre-Processing of Galaxies before Entering a Cluster. , 56:29–43.

Gunn, J. E. and Gott, J. Richard, I. (1972). On the Infall of Matter Into Clusters of Galaxies and Some Effects on Their Evolution. , 176:1.

Jaffé, Y. L., Smith, R., Candlish, G. N., Poggianti, B. M., Sheen, Y.-K., and Verheijen, M. A. W. (2015). BUDHIES II: a phase-space view of H I gas stripping and star formation quenching in cluster galaxies. , 448(2):1715–1728.

Kotecha, S., Welker, C., Zhou, Z., Wadsley, J., Kraljic, K., Sorce, J., Rasia, E., Roberts, I., Gray, M., Yepes, G., and Cui, W. (2022). Cosmic filaments delay quenching inside clusters. , 512(1):926–944.

Lintott, C., Schawinski, K., Bamford, S., Slosar, A., Land, K., Thomas, D., Edmondson, E., Masters, K., Nichol, R. C., Raddick, M. J., Szalay, A., Andreescu, D., Murray, P., and Vandenberg, J. (2011). Galaxy Zoo 1: data release of morphological classifications for nearly 900 000 galaxies. , 410(1):166–178.

Lintott, C. J., Schawinski, K., Slosar, A., Land, K., Bamford, S., Thomas, D., Raddick, M. J., Nichol, R. C., Szalay, A., Andreescu, D., Murray, P., and Vandenberg, J. (2008). Galaxy Zoo:

morphologies derived from visual inspection of galaxies from the Sloan Digital Sky Survey. , 389(3):1179–1189.

McPartland, C., Ebeling, H., Roediger, E., and Blumenthal, K. (2016). Jellyfish: the origin and distribution of extreme ram-pressure stripping events in massive galaxy clusters. , 455(3):2994–3008.

Peng, Y.-j., Lilly, S. J., Kovač, K., Bolzonella, M., Pozzetti, L., Renzini, A., Zamorani, G., Ilbert, O., Knobel, C., Iovino, A., Maier, C., Cucciati, O., Tasca, L., Carollo, C. M., Silverman, J., Kampczyk, P., de Ravel, L., Sanders, D., Scoville, N., Contini, T., Mainieri, V., Scodeggio, M., Kneib, J.-P., Le Fèvre, O., Bardelli, S., Bongiorno, A., Caputi, K., Coppa, G., de la Torre, S., Franzetti, P., Garilli, B., Lamareille, F., Le Borgne, J.-F., Le Brun, V., Mignoli, M., Perez Montero, E., Pello, R., Ricciardelli, E., Tanaka, M., Tresse, L., Vergani, D., Welikala, N., Zucca, E., Oesch, P., Abbas, U., Barnes, L., Bordoloi, R., Bottini, D., Cappi, A., Cassata, P., Cimatti, A., Fumana, M., Hasinger, G., Koekemoer, A., Leauthaud, A., Maccagni, D., Marinoni, C., McCracken, H., Memeo, P., Meneux, B., Nair, P., Porciani, C., Presotto, V., and Scaramella, R. (2010). Mass and Environment as Drivers of Galaxy Evolution in SDSS and zCOSMOS and the Origin of the Schechter Function. , 721(1):193–221.

Poggianti, B. M., Fasano, G., Omizzolo, A., Gullieuszik, M., Bettoni, D., Moretti, A., Paccagnella, A., Jaffé, Y. L., Vulcani, B., Fritz, J., Couch, W., and D'Onofrio, M. (2016). Jellyfish Galaxy Candidates at Low Redshift. , 151(3):78.

Schiminovich, D., Catinella, B., Kauffmann, G., Fabello, S., Wang, J., Hummels, C., Lemonias, J., Moran, S. M., Wu, R., Giovanelli, R., Haynes, M. P., Heckman, T. M., Basu-Zych, A. R., Blanton, M. R., Brinchmann, J., Budavári, T., Gonçalves, T., Johnson, B. D., Kennicutt, R. C., Madore, B. F., Martin, C. D., Rich, M. R., Tacconi, L. J., Thilker, D. A., Wild, V., and Wyder, T. K. (2010). The GALEX Arecibo SDSS Survey - II. The star formation efficiency of massive galaxies. , 408(2):919–934.

Springel, V., Frenk, C. S., and White, S. D. M. (2006). The large-scale structure of the Universe. , 440(7088):1137–1144.

Vulcani, B., Poggianti, B. M., Smith, R., Moretti, A., Jaffé, Y. L., Gullieuszik, M., Fritz, J., and Bellhouse, C. (2022). The Relevance of Ram Pressure Stripping for the Evolution of Blue Cluster Galaxies as Seen at Optical Wavelengths. , 927(1):91.

Willett, K. W., Lintott, C. J., Bamford, S. P., Masters, K. L., Simmons, B. D., Casteels, K. R. V., Edmondson, E. M., Fortson, L. F., Kaviraj, S., Keel, W. C., Melvin, T., Nichol, R. C., Raddick, M. J., Schawinski, K., Simpson, R. J., Skibba, R. A., Smith, A. M., and Thomas, D. (2013). Galaxy Zoo 2: detailed morphological classifications for 304 122 galaxies from the Sloan Digital Sky Survey. , 435(4):2835–2860.